Sodium Alginate–Derived Hydrophilic Gel@CuO Microspheres: A Green Nanocatalyst for Diverse Petasis Transformations with Antibacterial Activity

Nilesh T. Pandit[a], Avdhut D. Kadam[a], Avinash A. Survase[b], Komal R. Mali[c], Vishvanath B. Ghanwat[a], Sarika P. Patil[d,e], Chaitali S. Bagade[c], Tukaram Dongale[f,g], Santosh B. Kamble[d,e*]

[a] Department of Chemistry, Yashavantrao Chavan Institute of Science, constituent college, Karmaveer Bhaurao Patil University, Satara-415001, Maharashtra, India

[b] Department of Microbiology, Yashavantrao Chavan Institute of Science, constituent college, Karmaveer Bhaurao Patil University, Satara-415001, Maharashtra, India

[c] Department of Chemistry, Shivaji University Kolhapur, Maharashtra, India

[d] Department of Chemistry, Sadguru Gadage Maharaj College, Karad-415124, Maharashtra, India

[e] Karmaveer Bhaurao Patil University, Satara-415001, Maharashtra, India

[f] School of Nanoscience and Biotechnology, Shivaji University, Kolhapur-416004, Maharashtra, India

[g] School of Electrical Engineering, Korea University, Anam-ro 145, Seongbuk-gu, Seoul, Republic of Korea

Corresponding Author: Santosh Kamble

Email ID: santosh.san143@gmail.com

Orcid Id: 0000-0002-4668-1628

Supporting Data

INDEX

1. General

Experimental Procedure: -

Synthesis of Alkylaminophenols, indoline-derived arylglycines and Fused heterocycle derivatives -:

A mixture of the amine (1.0 mmol), aldehyde (1.0 mmol), and Gel@CuO microspheres (0.03g) was added to aqueous NaPTS solution (3 mL) and stirred for 5 min. Subsequently, the corresponding boronic acid was introduced, and the reaction mixture was stirred at room temperature until completion, as monitored by TLC. Upon completion, the reaction mixture was filtered to remove the catalyst, and the filtrate was subjected to standard purification procedures. The isolated products were characterized by ^{1}H and ^{13}C NMR spectroscopy.

2. Green Chemistry Matrix Calculations

To assess the environmental and operational efficiency of various synthetic routes to indoline-derived arylglycines, we calculated key green chemistry indicators for both our method and previously reported protocols, as detailed in Table 1. The parameters assessed include Reaction Mass Efficiency (RME, Equation 1), mass efficiency contributions from reactants, reagents, and catalyst (PMI_{RRC}), solvent-related mass input (PMI_{solv}), and overall Process Mass Intensity ($PMI_{total,}$ Equation 2)[1,2]. These calculations serve to objectively compare the sustainability and material economy of the methodologies under consideration.

$$\text{RME:} \quad \frac{\text{Actual mass of product}}{\text{Sum of mass of all reactants utilized in reaction}} \text{ X } 100 \qquad (1)$$

$$\text{PMI:} \quad \frac{\text{Mass of all input materials}}{\text{Actual mass of product}} \qquad (2)$$

Table 1: Green chemistry metrics for Gel@CuO-catalyzed Petasis reactions, including solvent PMI (PMI_{solv}), reactant-related PMI (PMI_{RRC}), total PMI (PMI_{total}), reaction mass efficiency (RME), and isolated yields for all synthesized derivatives.

Experimental Data						Experimental Data					
Entry	**PMI_{solv} (g g-1)**	**PMI_{RRC} (g g-1)**	**PMI_{total} (g g-1)**	**RME (%)**	**Yield (%)**	**Entry**	**PMI_{solv} (g g-1)**	**PMI_{RRC} (g g-1)**	**PMI_{total} (g g-1)**	**RME (%)**	**Yield (%)**
1	10.3	2.3	12.6	80	96	**14**	11.2	2.4	13.6	77	94
2	9.7	2.2	11.9	81	97	**15**	9.3	2.2	11.5	80	94
3	9.1	2.1	11.2	84	99	**16**	10.9	2.5	13.4	73	88
4	10.5	2.4	12.9	77	92	**17**	11.6	2.5	14.1	78	96
5	9.4	2.3	11.7	77	90	**18**	10.2	2.3	12.5	81	98
6	10.6	2.3	12.9	78	94	**19**	11.1	2.4	13.5	79	96
7	7.4	1.9	9.3	85	98	**20**	10.4	2.3	12.7	80	97

8	7.3	1.9	9.2	84	96	**21**	7.5	1.9	9.4	85	98
9	10.4	2.3	12.7	80	96	**22**	9.3	4.1	13.4	79	98
10	11.1	2.4	13.6	78	95	**23**	10.5	4.5	14.9	76	96
11	10.8	2.4	13.2	78	94	**24**	8.8	4.0	12.8	74	86
12	10.4	2.3	12.7	80	96	**25**	14.9	3.3	18.2	56	92.0
13	10.4	2.4	12.7	76	96	**26**	12.3	2.8	15.1	62	98
	-	-	-	-	-	**27**	13.4	16.4	3.0	59	96.0

The green chemistry performance of the Gel@CuO catalyzed Petasis reactions was evaluated using key quantitative metrics, including solvent Process Mass Intensity (PMI_{solv}), reactant-related PMI (PMI_{RR}), total PMI (PMI_{total}), Reaction Mass Efficiency (RME), and isolated yield (Table 1). Across most entries (1–21), corresponding to alkylaminophenol derivatives, the reactions exhibit low PMI_{total} values (9.2–14.1 g g^{-1}) along with high RME (77–85%) and excellent yields (90–99%), indicating efficient material utilization and minimal waste generation under aqueous NaPTS conditions. Notably, entries 7, 8, and 21 show the lowest PMI_{total} (~9.2–9.4 g g^{-1}) combined with high RME (~85%) and yields (~98%), highlighting particularly sustainable transformations, likely due to faster reaction rates and reduced solvent demand.

For arylglycine derivatives (entries 22–23) and the pyridine-based derivative (entry 24), a moderate increase in PMI_{RRC} and PMI_{total} (12.8–14.9 g g^{-1}) is observed, which can be attributed to the higher molecular weights and additional stoichiometric contributions of heteroaryl substrates. Nevertheless, these reactions still maintain high yields (86–98%), reflecting the robustness of the Gel@CuO catalyst. In contrast, fused morpholine derivatives (entries 25–27) display comparatively higher PMI_{total} values (15.1–18.2 g g^{-1}) and lower RME (56–62%), consistent with their increased structural complexity and multiring frameworks, which inherently reduce mass efficiency. Despite this, the yields remain high (92–98%), demonstrating that catalytic efficiency is preserved even for more demanding substrates. Overall, the consistently low PMI values, high RME, and excellent product yields across a broad substrate scope confirm that

the Gel@CuO microsphere-catalyzed Petasis reaction operates within a favorable green chemistry matrix, effectively minimizing solvent and material inputs while maximizing product output. These results underscore the sustainability advantage of combining a recyclable biopolymer-based nanocatalyst with an aqueous hydrotropic medium for multicomponent synthesis.

3. Atom Economy

The atom economy values for the synthesized Petasis reaction products (Table 2) were calculated to evaluate the intrinsic material efficiency of the Gel@CuO-catalyzed multicomponent process. Most alkylaminophenol derivatives (4a–4x) exhibit high atom economy values in the range of 79–87%, reflecting the favorable nature of the Petasis reaction, in which the majority of atoms from the aldehyde, amine, and boronic acid are incorporated into the final product. Notably, derivatives such as 4g, 4h, 4u, and 4x show the highest atom economy (≈86–87%), indicating minimal generation of stoichiometric by-products and excellent atom utilization.

In contrast, comparatively lower atom economy values were observed for structurally more complex derivatives, particularly 4y, 4z, and $4Z_1$ (60–63%) (Figure 1). This decrease can be attributed to the involvement of additional functional groups and ring-forming steps, which inherently increase molecular complexity and reduce the proportion of reactant atoms retained in the target molecule. Nevertheless, even for these derivatives, the atom economy remains acceptable for multicomponent reactions, highlighting the efficiency of the Gel@CuO catalytic system. Overall, the consistently high atom economy across the majority of products confirms that the present methodology aligns well with the principles of green chemistry, emphasizing efficient atom utilization, reduced waste generation, and sustainable synthesis of diverse Petasis reaction derivatives.

Table 2: Atom economy values (%) for the Gel@CuO catalyzed Petasis reaction products (4a–$4Z_1$), highlighting efficient incorporation of reactant atoms into the final molecules.

Products	Atom Economy	Products	Atom Economy
4a	83	**4n**	82
4b	84	**4o**	85
4c	84	**4p**	83
4d	83	**4q**	81
4e	85	**4r**	83
4f	83	**4s**	82
4g	87	**4t**	83
4h	87	**4u**	87
4i	83	**4v**	80
4j	82	**4w**	79
4k	83	**4x**	86

4l	83	**4y**	60
4m	79	**4z**	63
-	**-**	**4Z$_1$**	62

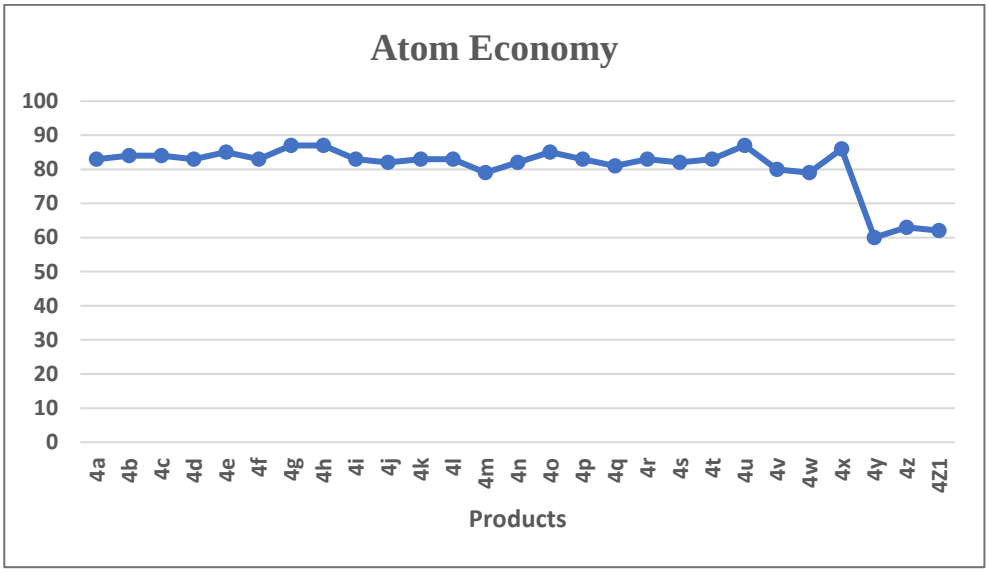

Fig. 1 Atom economy (%) of Petasis reaction products (4a–4Z$_1$) synthesized using the Gel@CuO microsphere catalyst, illustrating the high material efficiency of the multicomponent protocol.

4. Spectral data:

Compound-1(Table-3, Entry-12)

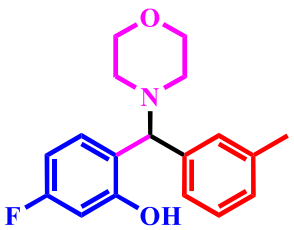

5-fluoro-2-(morpholino(*m*-tolyl)methyl)phenol

FT-IR:

IR (KBr): ν_{max}: 3415, 2976, 1961, 1727, 1549, 1390, 1067, 1004, 718.

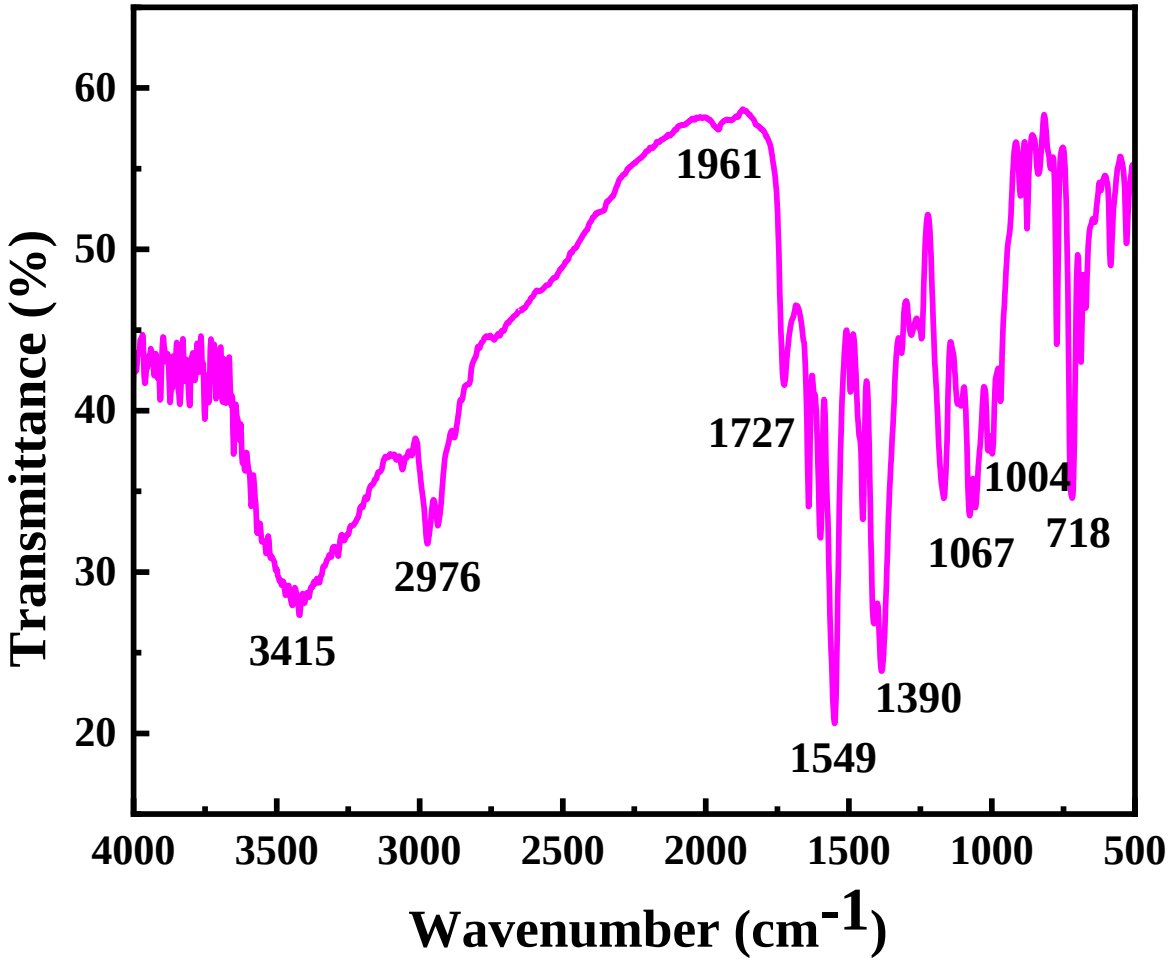

Fig. 2 FT-IR spectrum of 5-fluoro-2-(morpholino(m-tolyl)methyl)phenol (Table-4, Entry-12)

^{1}H NMR:

^{1}H NMR (400 MHz, $CDCl_3$) δ 12.00 (s, 1H), 7.12 (t, *J* = 6.5 Hz, 3H), 7.05 – 6.98 (m, 1H), 6.82 – 6.74 (m, 2H), 6.63 (dd, *J* = 8.1, 2.1 Hz, 1H), 4.29 (s, 1H), 3.76 – 3.61 (m, 4H), 2.72 – 2.30 (m, 4H), 2.25 (s, 3H).

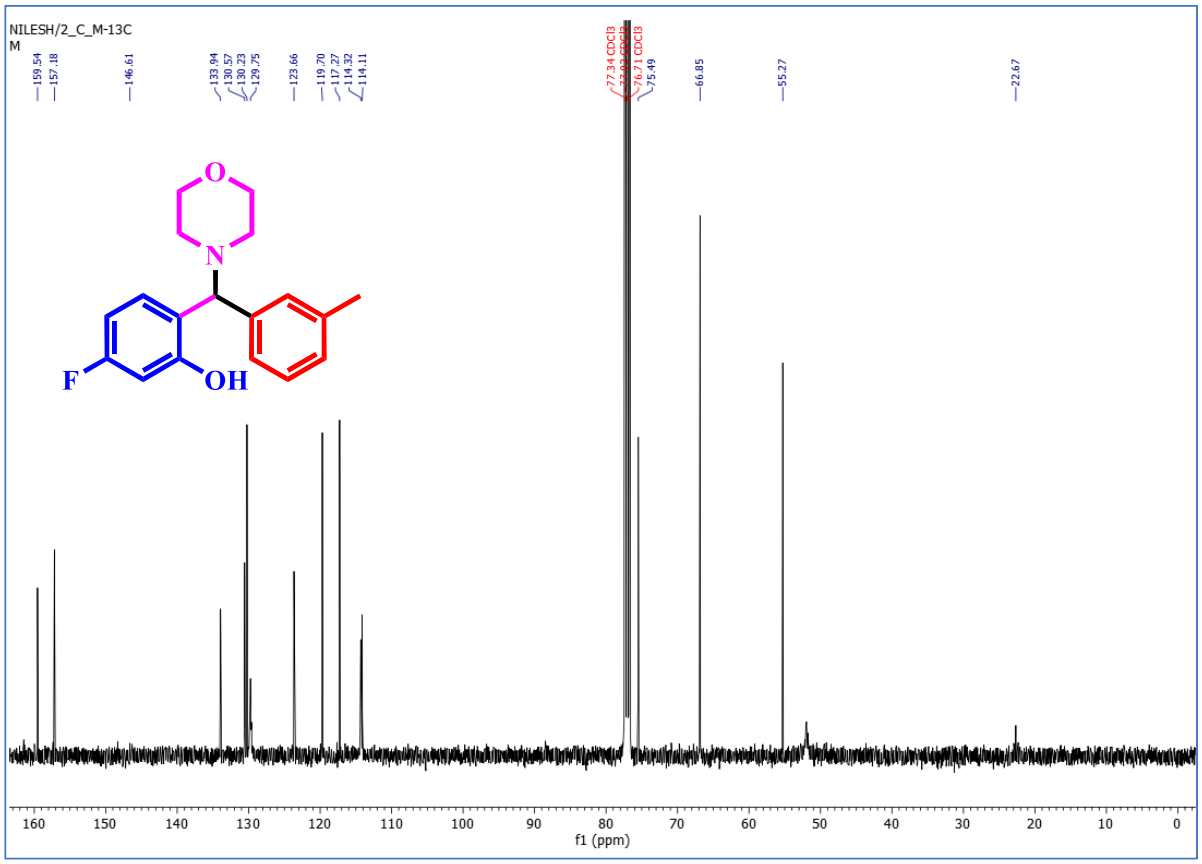

Fig. 3 ^{1}H NMR spectrum of 5-fluoro-2-(morpholino(m-tolyl)methyl)phenol

^{13}C NMR: -

^{13}C NMR (101 MHz, $CDCl_3$) δ 159.54, 157.18, 146.61, 133.94, 130.57, 130.23, 129.75, 123.66, 119.70, 117.27, 114.32, 114.11, 75.49, 66.85, 55.27, 22.67.

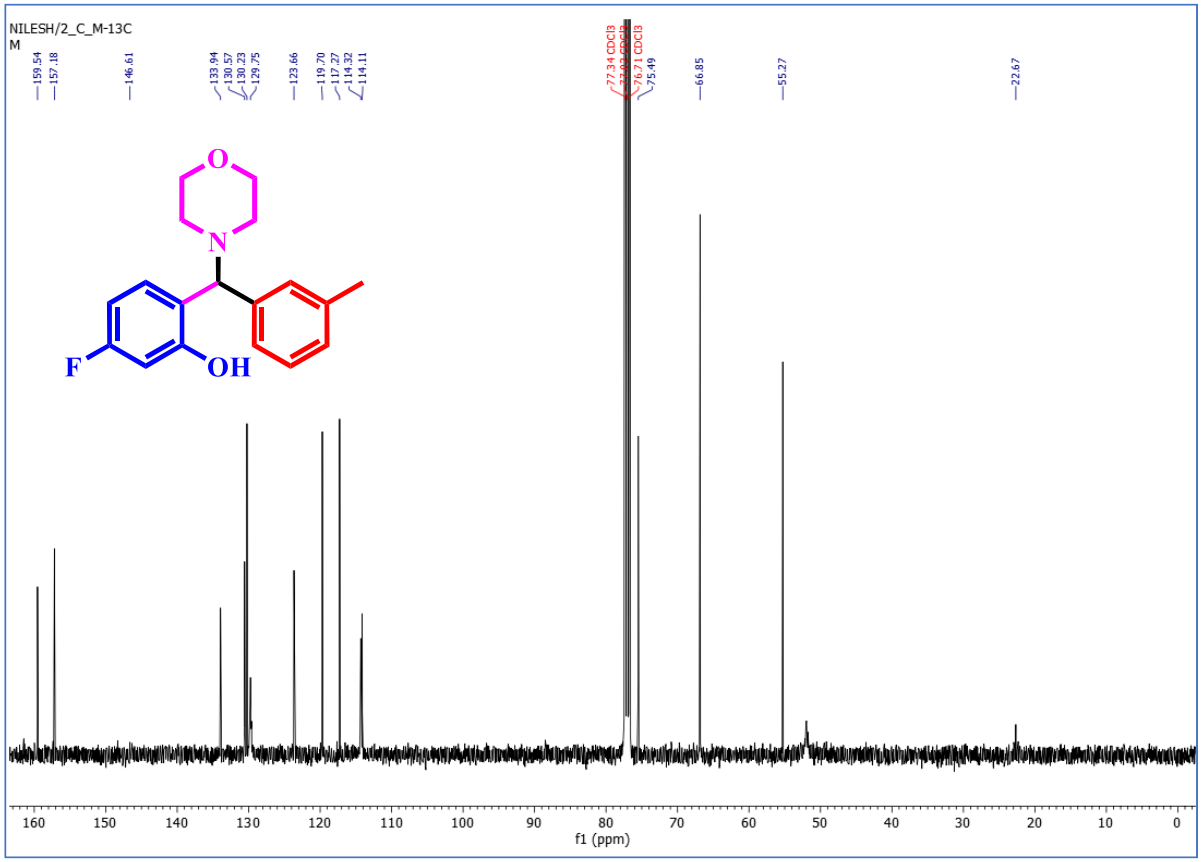

Fig. 4 ^{13}C NMR spectrum of 5-fluoro-2-(morpholino(m-tolyl)methyl)phenol

Compound-2(Table-3, Entry-3)

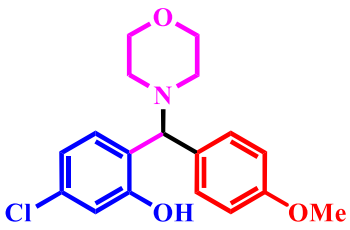

5-chloro-2-((4-methoxyphenyl)(morpholino)methyl)phenol

FT-IR:

IR (KBr): ν_{max}: - 3395, 2957, 2355, 1727, 1619, 1511, 1384, 1067, 991, 744

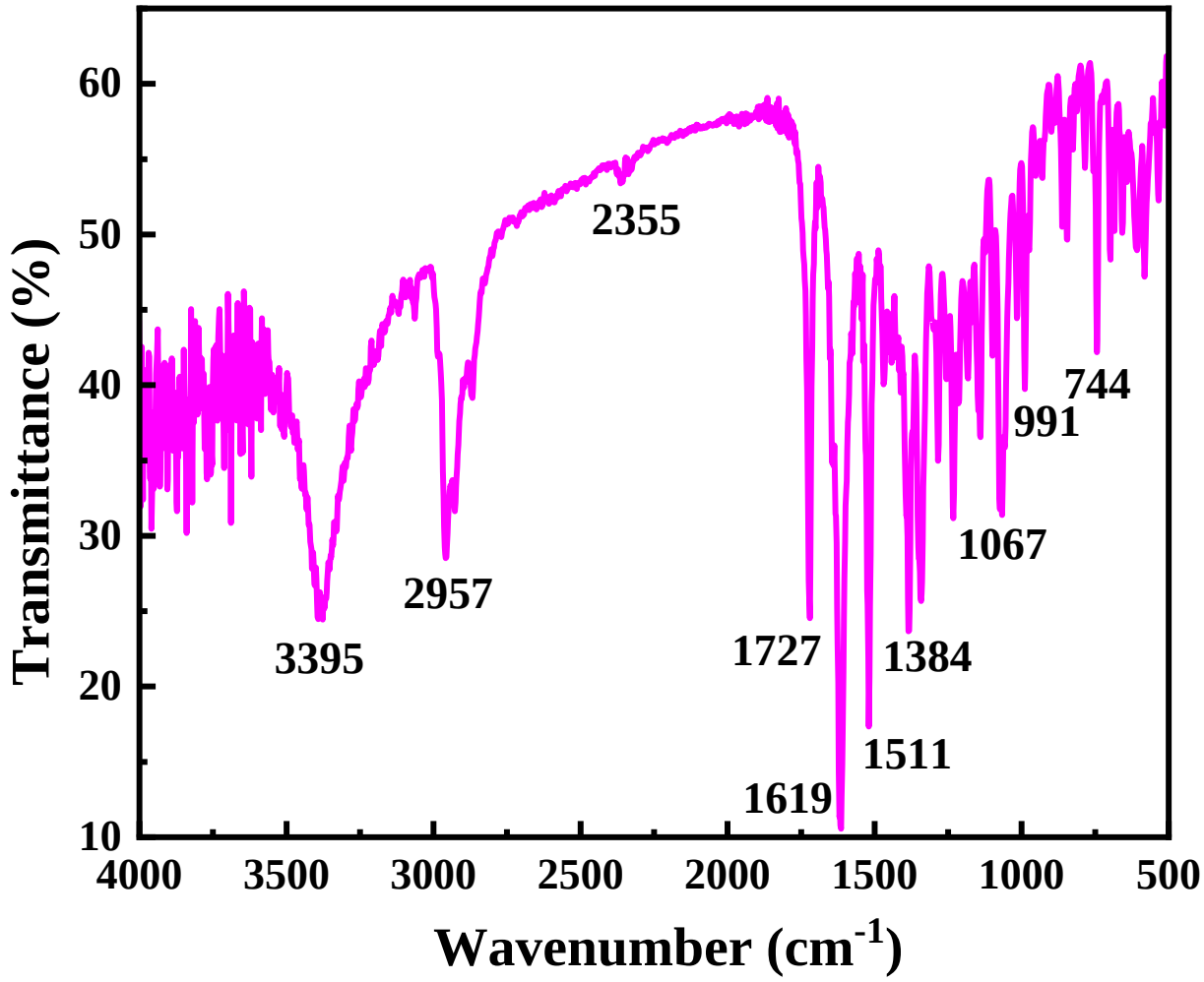

Fig. 5 FT-IR spectrum of 5-chloro-2-((4-methoxyphenyl)(morpholino)methyl)phenol (Table-3, Entry-3)

^{1}H NMR:

^{1}H NMR (400 MHz, $CDCl_3$) δ 12.09 (s, 1H), 7.22 (d, *J* = 8.1 Hz, 2H), 6.77 (d, *J* = 3.6 Hz, 2H), 6.63 (dd, *J* = 8.2, 2.1 Hz, 2H), 4.30 (s, 1H), 3.68 (s, 4H), 2.57 – 2.23 (m, 4H).

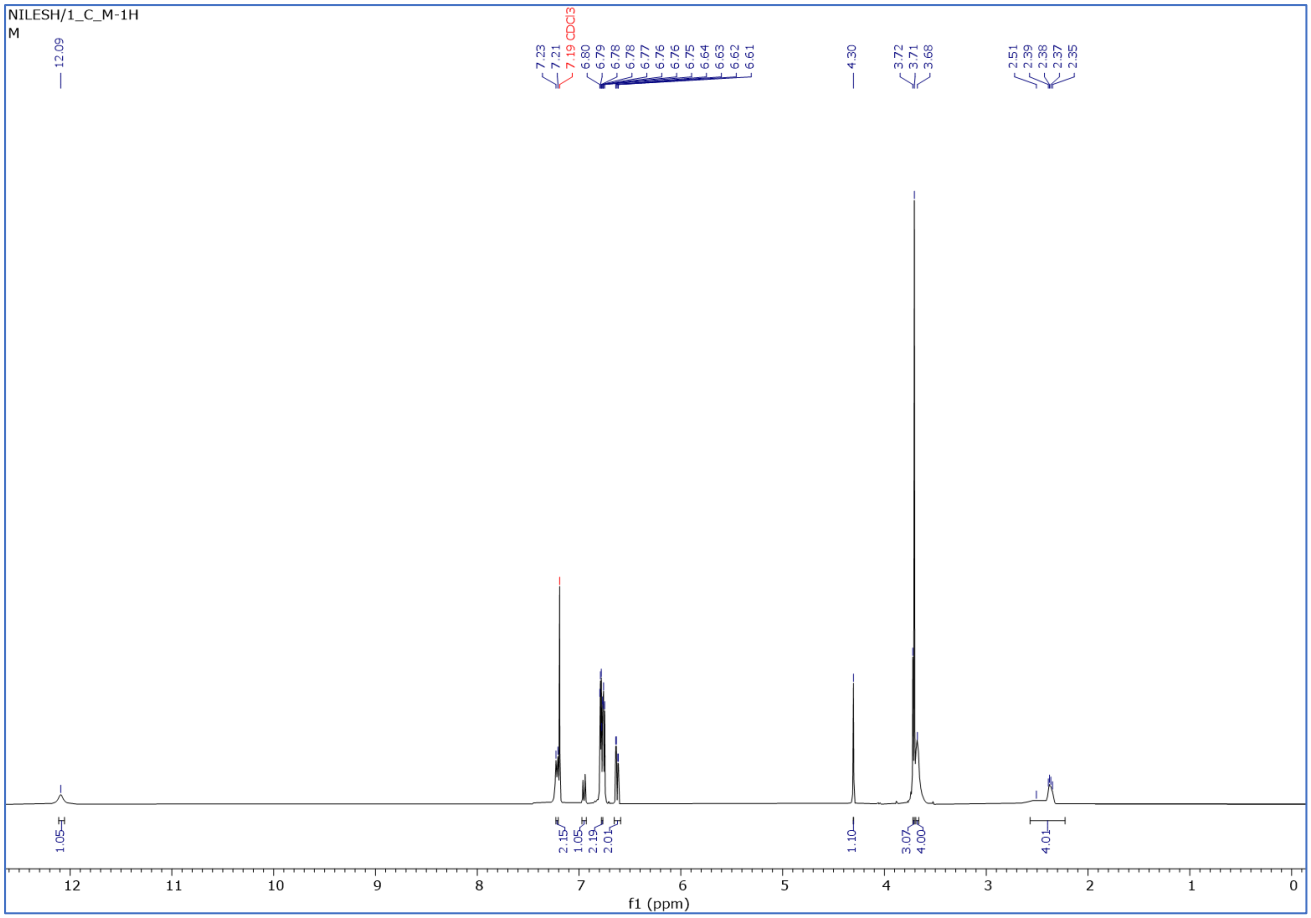

Fig. 6 ^{1}H NMR spectrum of 5-chloro-2-((4-methoxyphenyl)(morpholino)methyl)phenol

^{13}C NMR: -

^{13}C NMR (101 MHz, $CDCl_3$) δ 159.54, 157.18, 133.94, 130.57, 130.23, 129.76, 129.57, 123.66, 119.70, 117.27, 114.31, 75.49, 66.85, 55.27, 49.14.

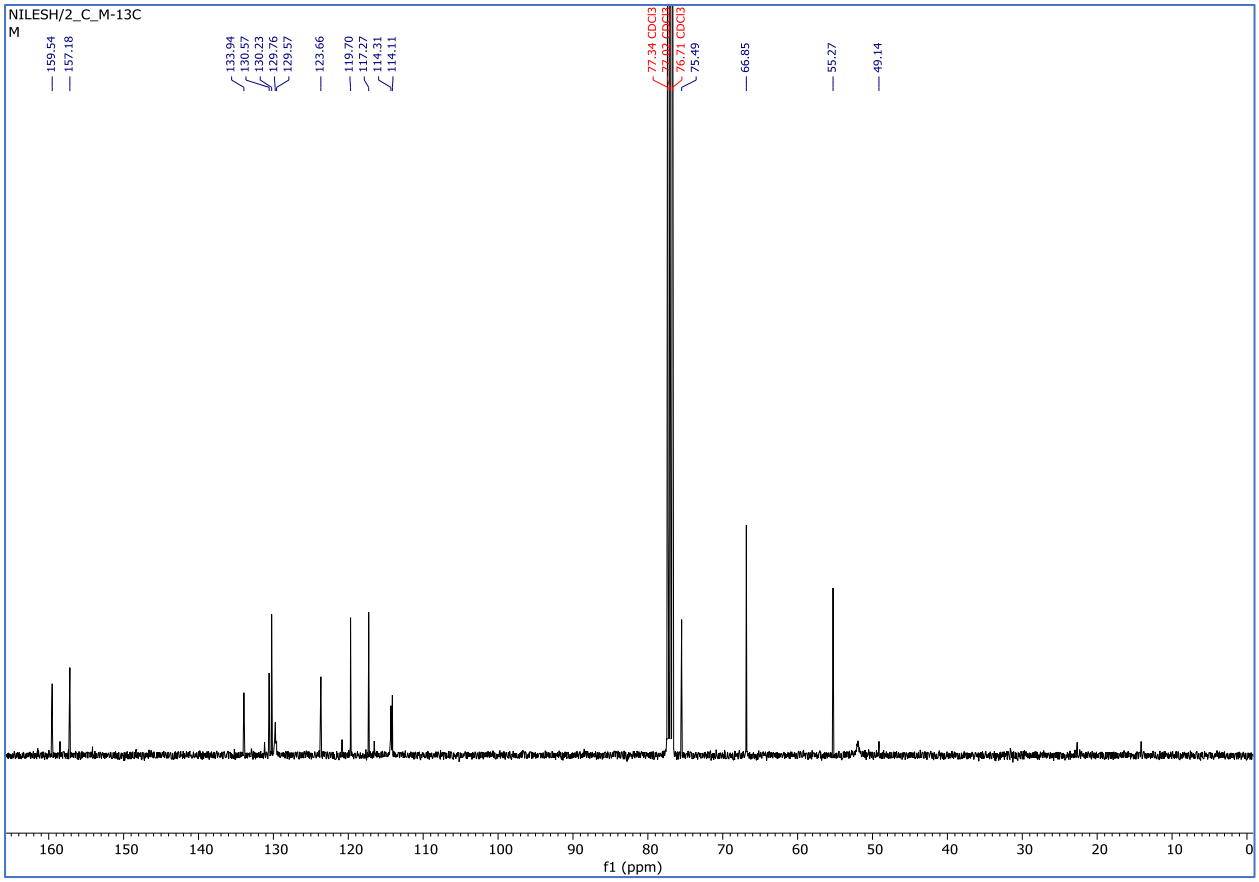

Fig. 7 ^{13}C NMR spectrum of 5-chloro-2-((4-methoxyphenyl)(morpholino)methyl)phenol

Compound-3(Table-3, Entry-7)

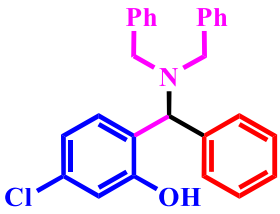

5-chloro-2-((dibenzylamino)(phenyl)methyl)phenol

FT-IR: -

IR (KBr): ν_{max}: 3450, 2928, 2354, 1629, 1518, 1342, 1036, 800, 526.

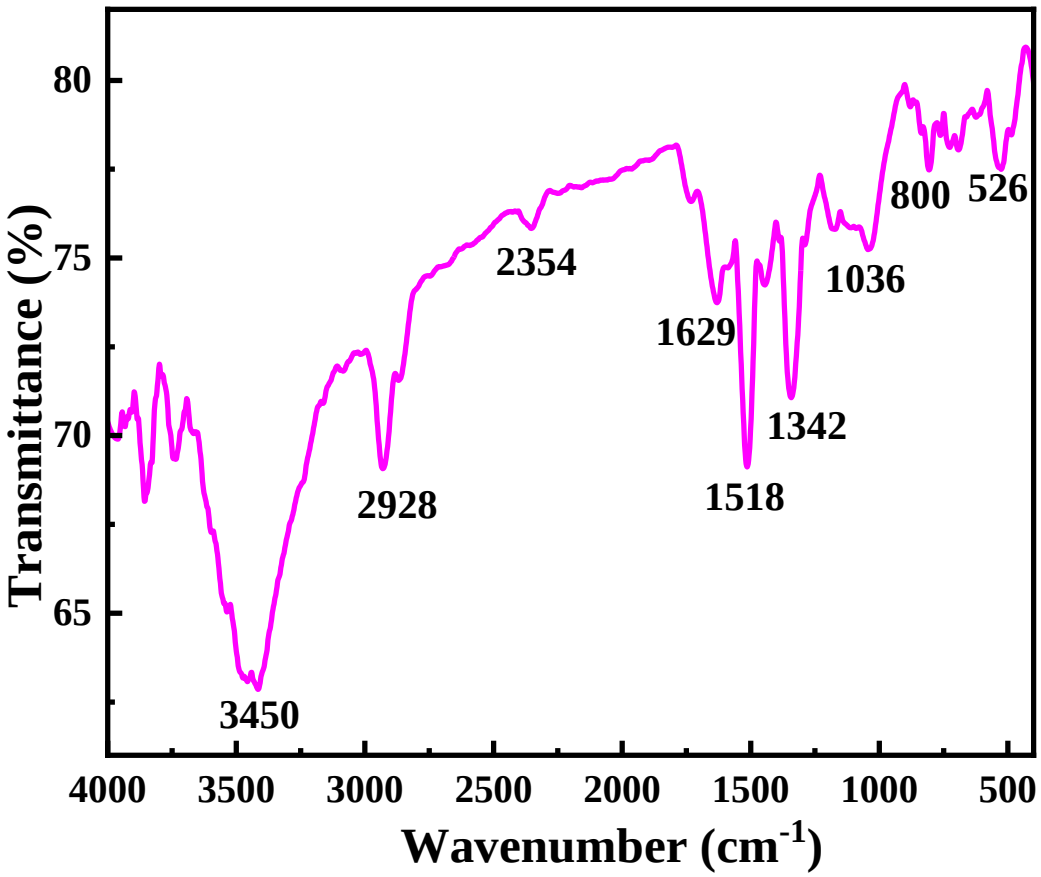

Fig. 8 FT-IR spectrum of 5-chloro-2-((dibenzylamino)(phenyl)methyl)phenol (Table-3, Entry-7)

^{1}H NMR:

^{1}H NMR (400 MHz, $CDCl_3$) δ 12.41 (s, 1H), 7.36 (ddt, *J* = 10.7, 9.0, 3.2 Hz, 3H), 7.32 – 7.25 (m, 6H), 7.21 (td, *J* = 6.7, 1.8 Hz, 6H), 6.86 (d, *J* = 1.9 Hz, 1H), 6.68 – 6.56 (m, 2H), 5.03 (s, 1H), 3.86 (d, *J* = 13.2 Hz, 2H), 3.29 (d, *J* = 13.3 Hz, 2H).

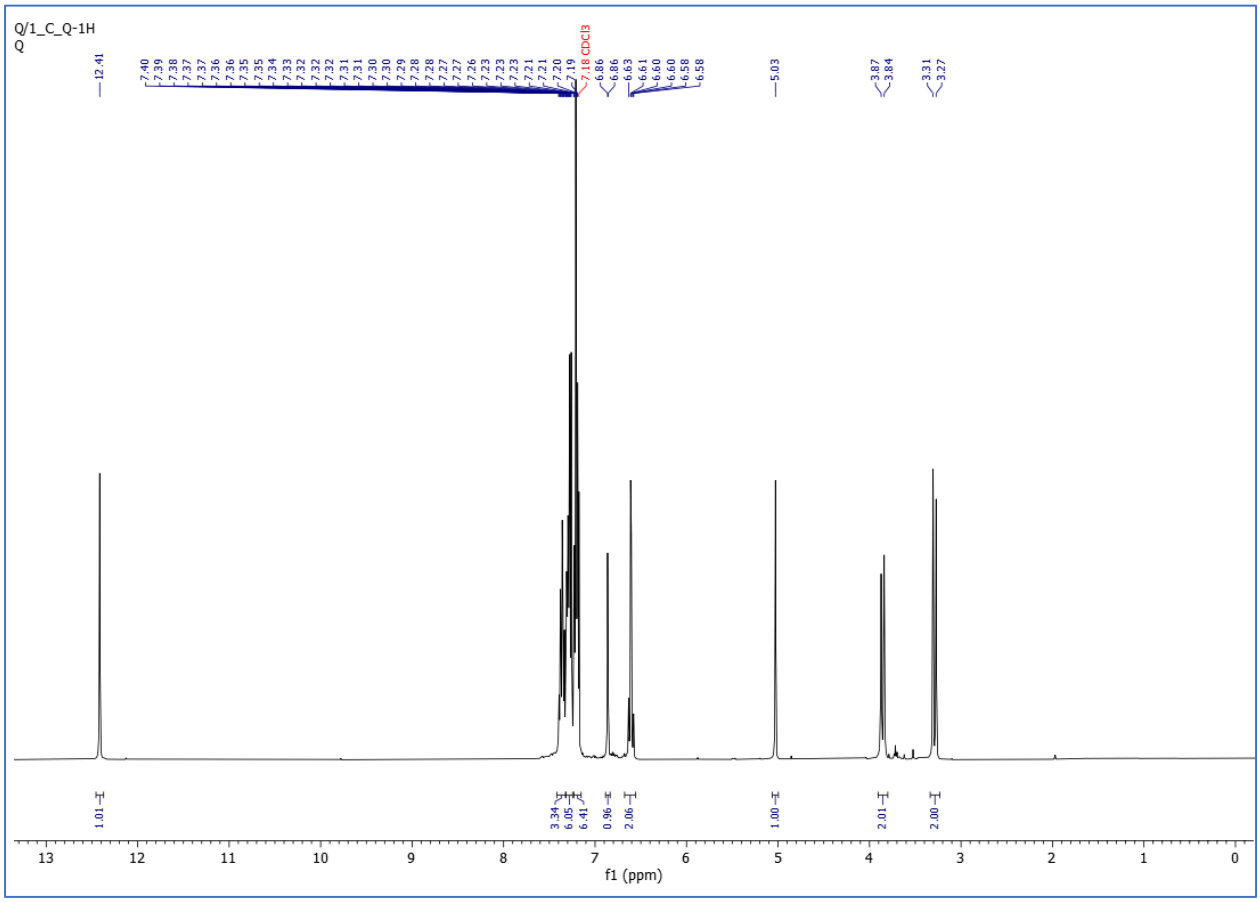

Fig. 9 ^{1}H NMR spectrum of 5-chloro-2-((dibenzylamino)(phenyl)methyl)phenol

^{13}C NMR: -

^{13}C NMR (101 MHz, $CDCl_3$) δ 158.55, 136.66, 134.98, 134.24, 130.63, 130.55, 129.78, 128.73, 128.71, 128.54, 127.76, 123.10, 119.09, 116.95, 77.24, 67.75, 53.78.

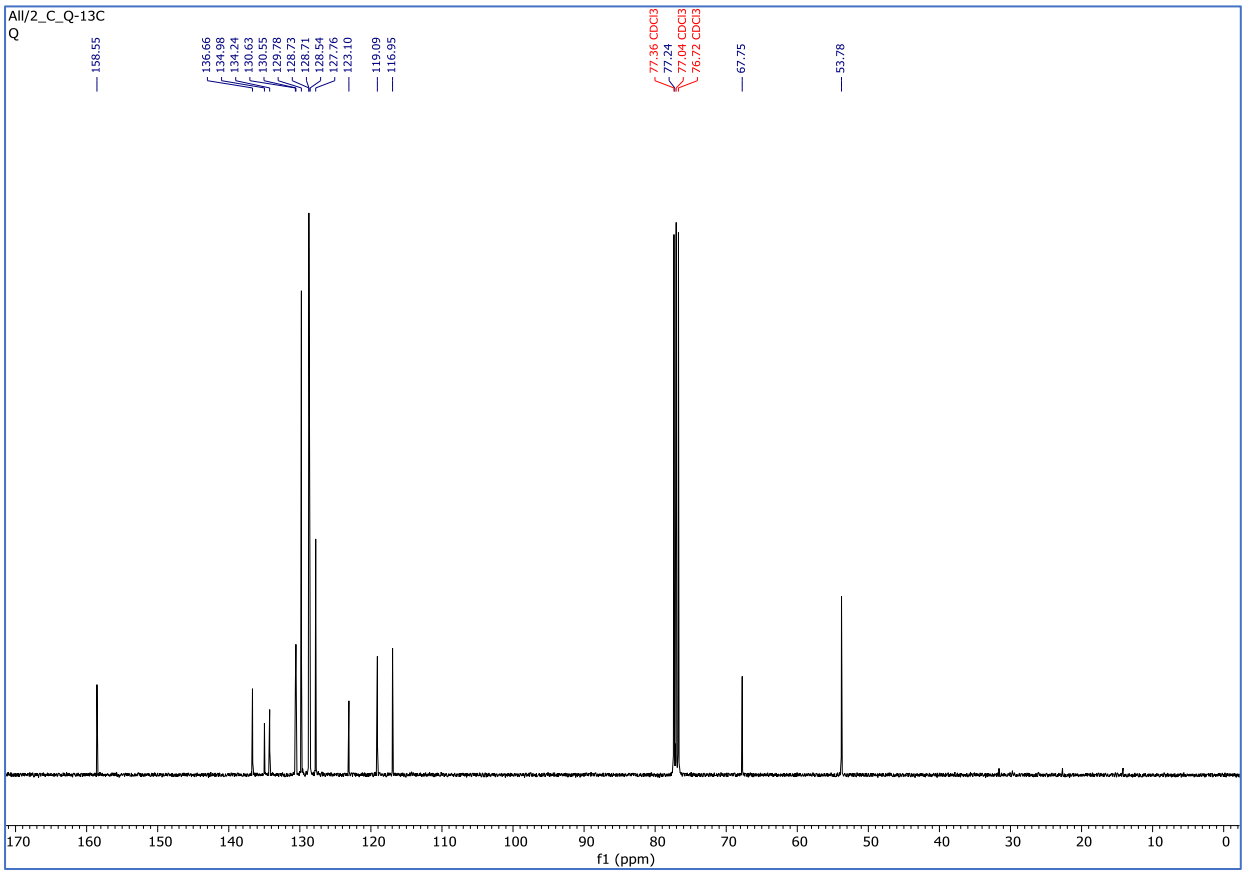

Fig. 10 ^{13}C NMR spectrum of 5-chloro-2-((dibenzylamino)(phenyl)methyl)phenol

Compound-4(Table-3, Entry-26)

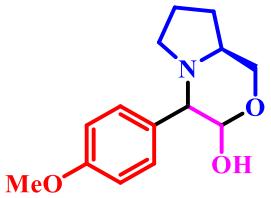

(8a*S*)-4-(4-methoxyphenyl)hexahydro-1*H*-pyrrolo[2,1-*c*][1,4]oxazin-3-ol

FT-IR: -

IR (KBr): ν_{max}: 3456, 2934, 2360, 1916, 1636, 1525, 1342, 1029, 793, 546.

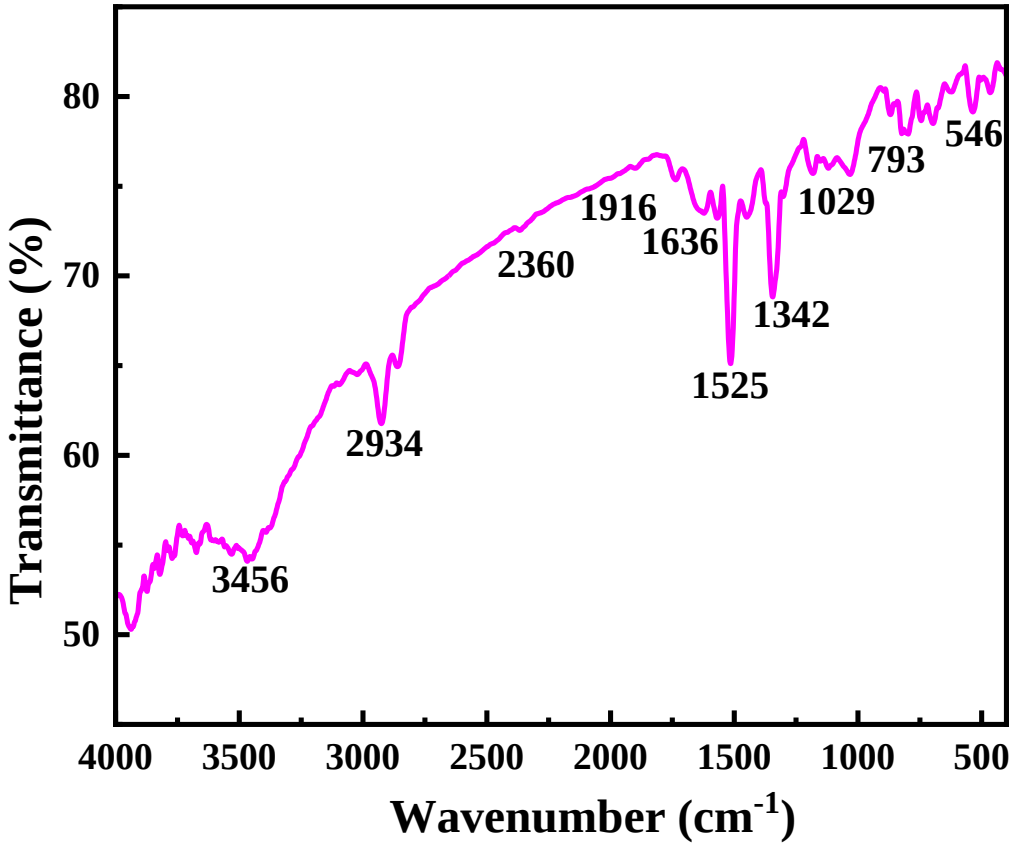

Fig. 11 FT-IR spectrum of (8aS)-4-(4-methoxyphenyl)hexahydro-1H-pyrrolo[2,1-c][1,4]oxazin-3-ol (Table-3, Entry-26)

^{1}H NMR

^{1}H NMR (400 MHz, $CDCl_3$) δ 7.39 – 7.30 (m, 2H), 6.86 – 6.79 (m, 2H), 5.03 (d, *J* = 2.6 Hz, 1H), 4.19 (dd, *J* = 11.2, 3.6 Hz, 1H), 3.98 – 3.82 (m, 2H), 3.82 – 3.77 (m, 1H), 3.74 (s, 3H), 2.77 – 2.70 (m, 1H), 2.68 – 2.53 (m, 1H), 2.26 – 2.14 (m, 1H), 1.76 – 1.51 (m, 4H).

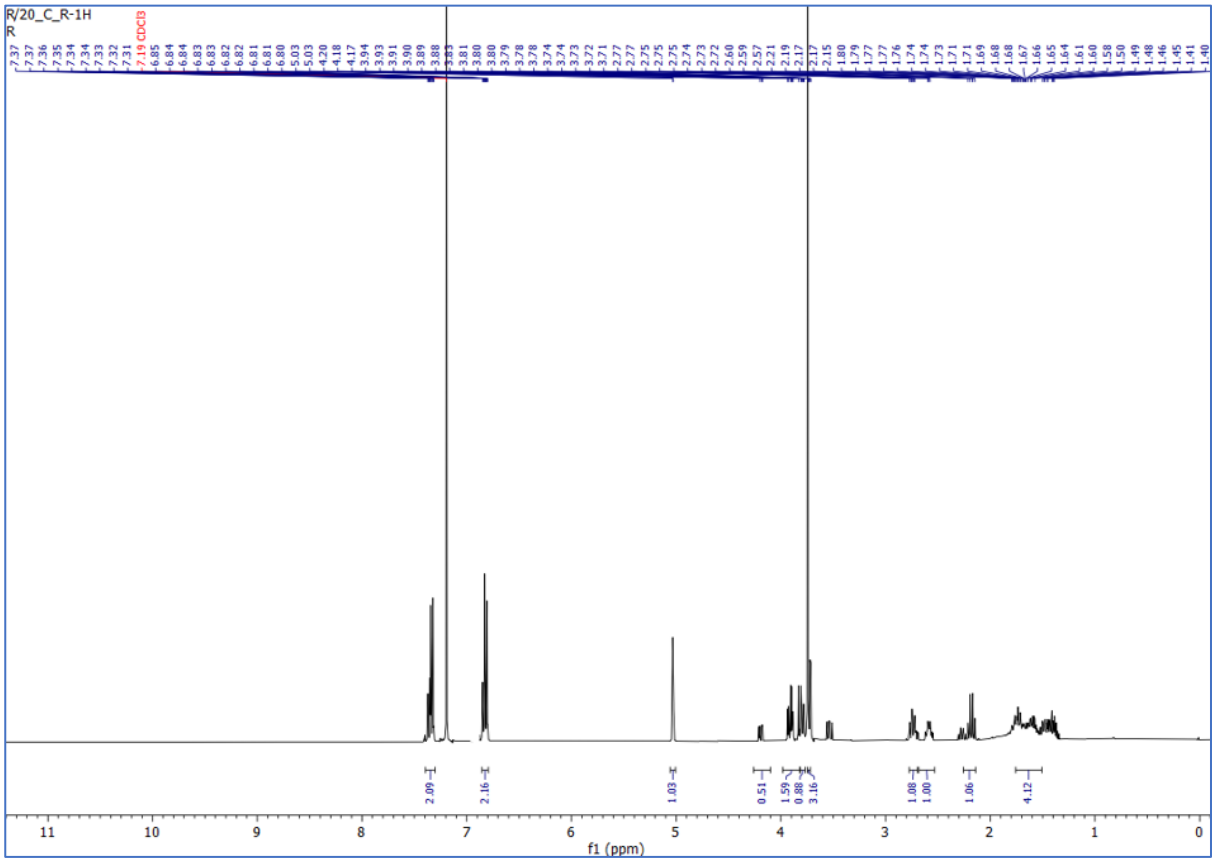

Fig. 12 ^{1}H NMR spectrum of (8aS)-4-(4-methoxyphenyl)hexahydro-1H-pyrrolo[2,1-c][1,4]oxazin-3-ol

^{13}C NMR

^{13}C NMR (101 MHz, $CDCl_3$) δ 159.14, 141.47, 131.32, 131.24, 113.86, 113.32, 97.04, 64.54, 63.96, 55.22, 53.73, 49.68, 25.71, 21.59.

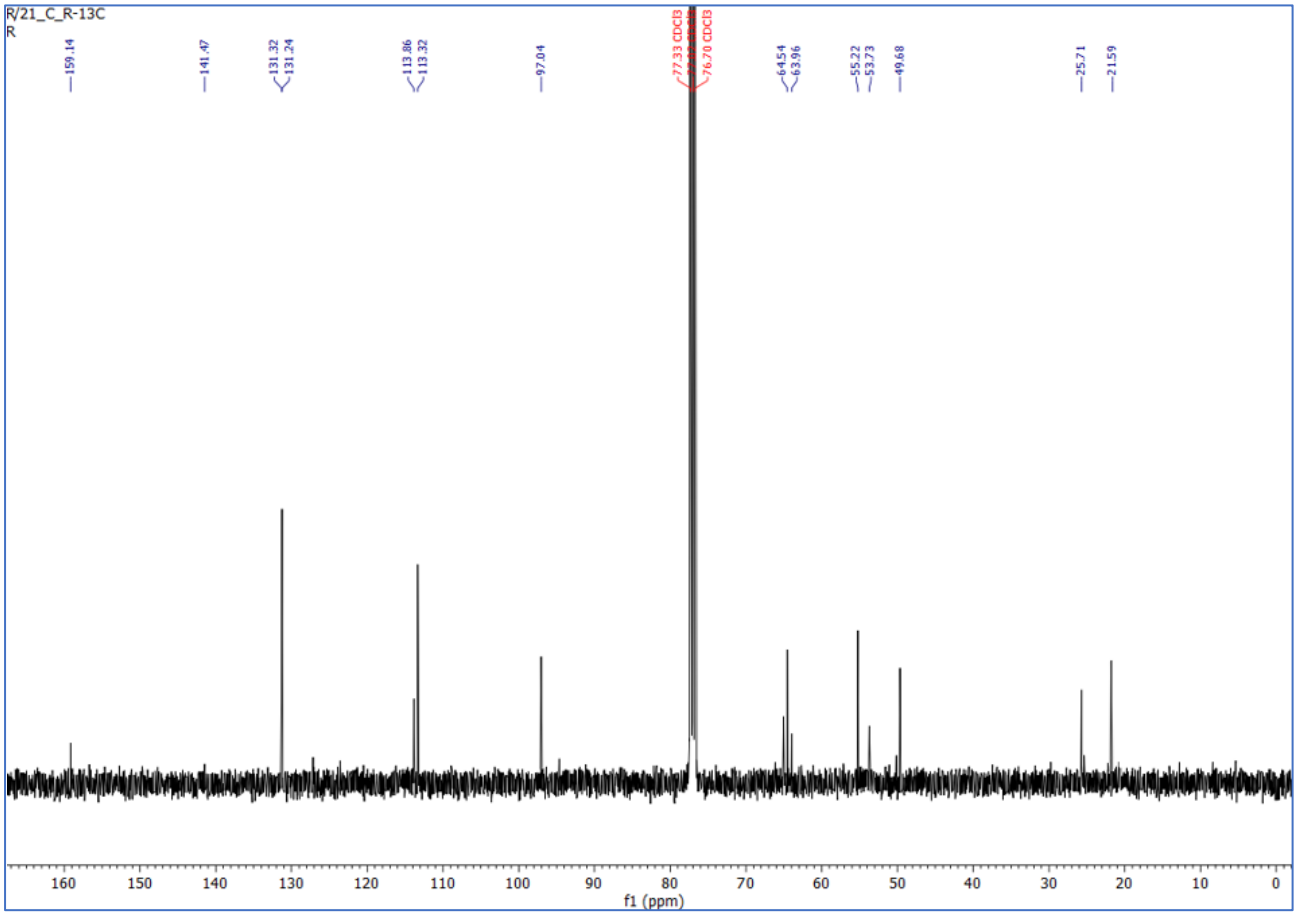

Fig. 13 ^{13}C NMR spectrum of (8aS)-4-(4-methoxyphenyl)hexahydro-1H-pyrrolo[2,1-c][1,4]oxazin-3-ol

Compound-5(Table-3, Entry-24)

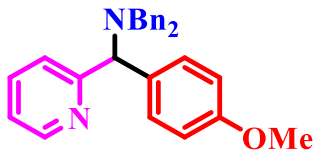

***N*,*N*-dibenzyl-1-(4-methoxyphenyl)-1-(pyridin-2-yl)methanamine**

FT-IR:

IR (KBr): ν_{max}: - 3440, 2964, 2647, 1708, 1590, 1365, 1263, 1145, 853, 591.

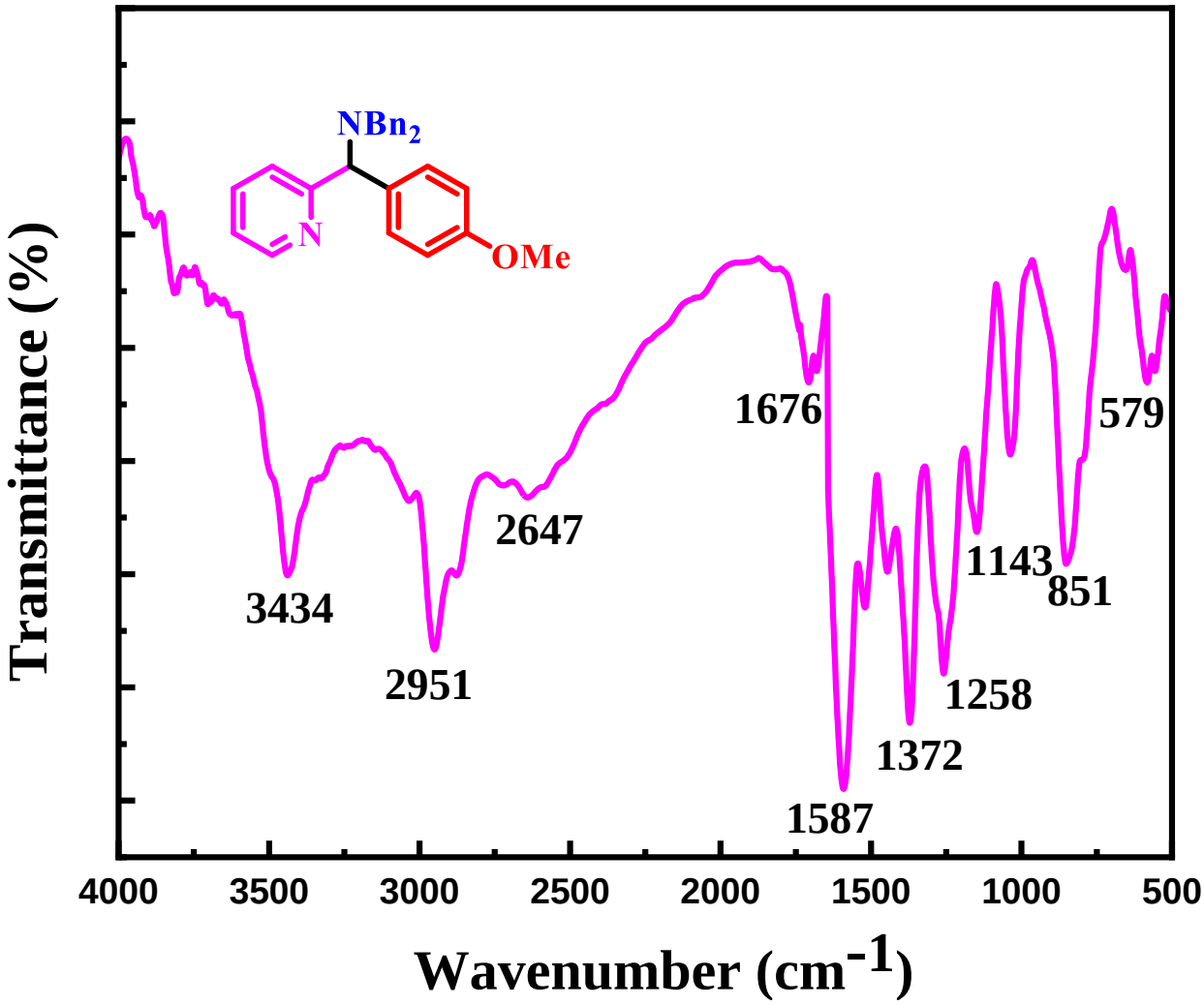

Fig. 14 FT-IR spectrum of N,N-dibenzyl-1-(4-methoxyphenyl)-1-(pyridin-2-yl)methanamine (Table-3, Entry-24)

^{1}H NMR

^{1}H NMR (400 MHz, $CDCl_3$) δ 8.62 (d, J = 4.9 Hz, 1H), 7.68 – 7.55 (m, 2H), 7.41 – 7.29 (m, 10H), 7.24 (t, J = 7.2 Hz, 2H), 7.19 – 7.13 (m, 1H), 6.89 (d, J = 8.4 Hz, 2H), 5.07 (s, 1H), 3.85 (d, J = 31.3 Hz, 4H), 3.69 (s, 3H).

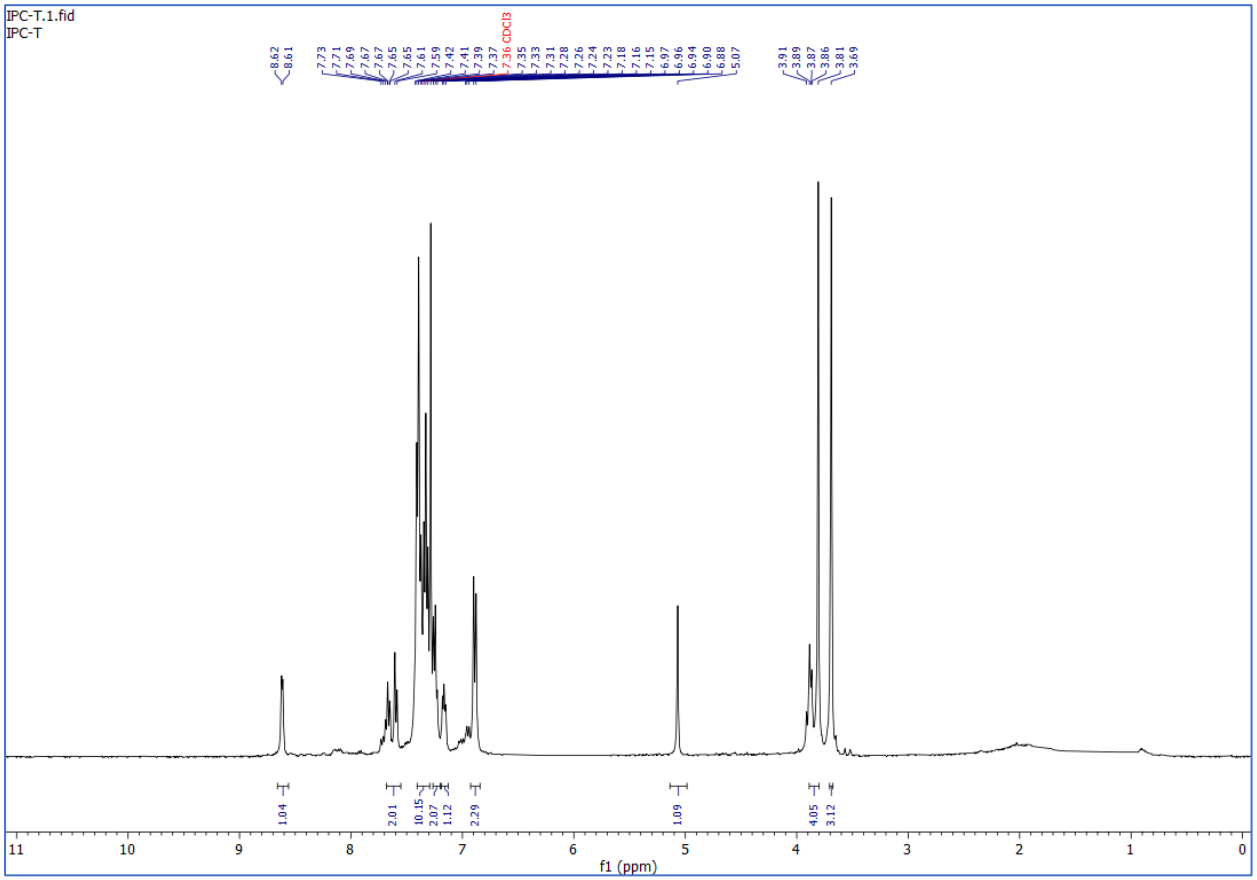

Fig. 15 ^{1}H NMR spectrum of N,N-dibenzyl-1-(4-methoxyphenyl)-1-(pyridin-2-yl)methanamine

^{13}C NMR

^{13}C NMR (101 MHz, $CDCl_3$) δ 161.61, 158.65, 149.03, 139.45, 136.16, 132.34, 130.20, 128.80, 128.22, 126.77, 123.42, 121.79, 113.65, 77.22, 69.08, 55.22, 53.92.

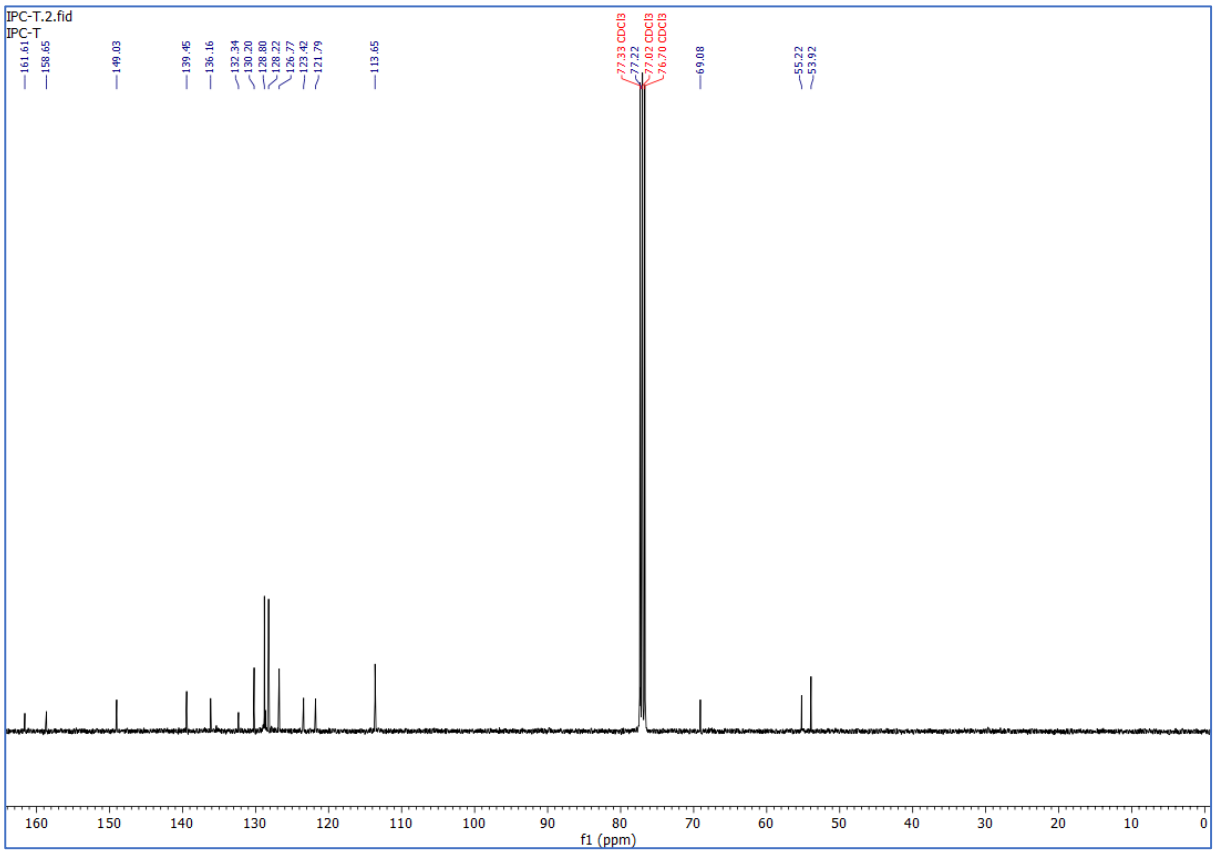

Fig. 16 ^{13}C NMR spectrum of N,N-dibenzyl-1-(4-methoxyphenyl)-1-(pyridin-2-yl)methanamine

Compound-6(Table-3, Entry-17)

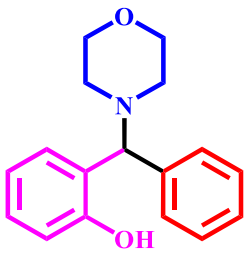

2-(morpholino(phenyl)methyl)phenol

FT-IR: -

IR (KBr): ν_{max}:

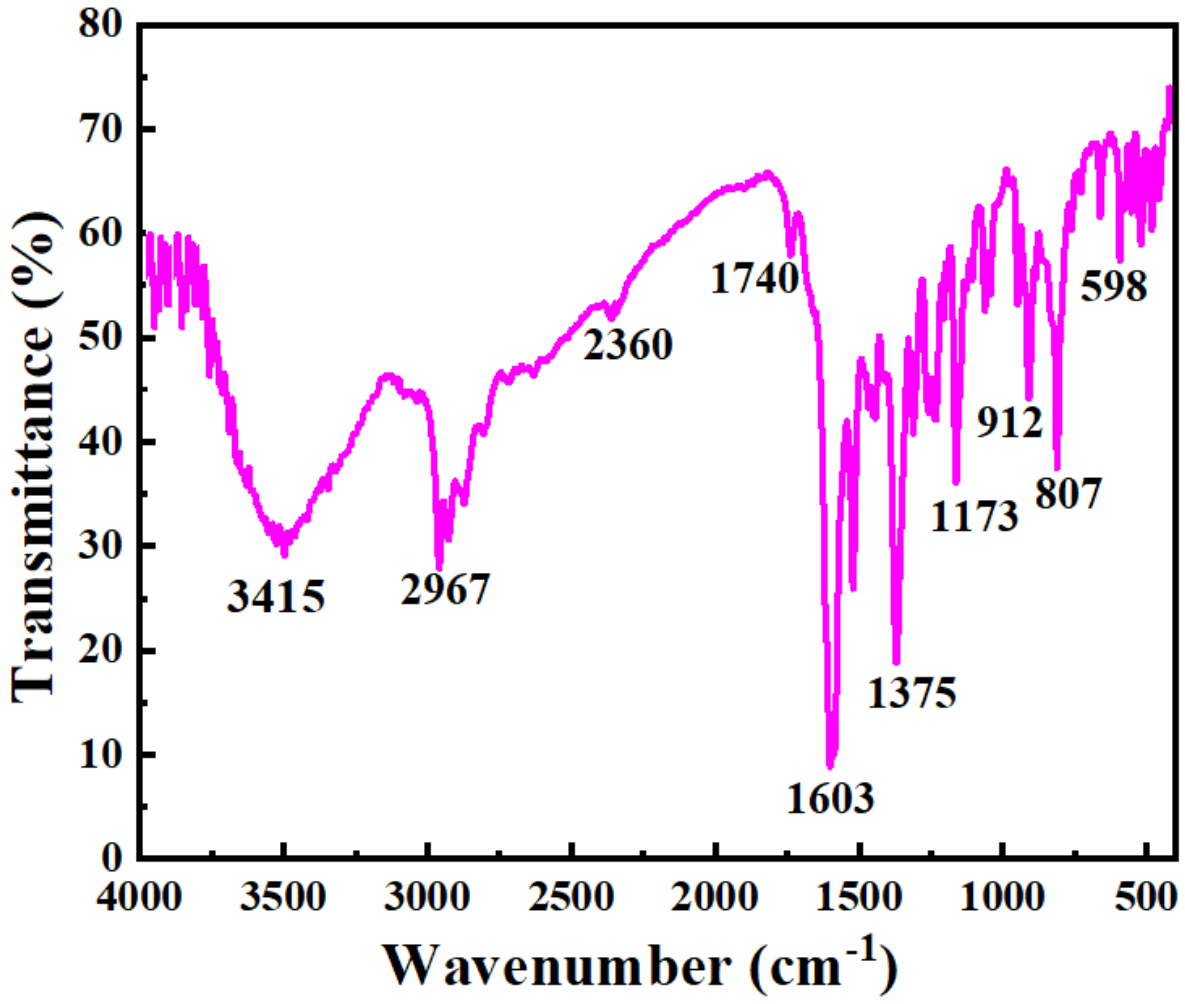

Fig. 17 FT-IR spectrum of 2-(morpholino(phenyl)methyl)phenol (Table-3, Entry-17)

^{1}H NMR

^{1}H NMR (400 MHz, $CDCl_3$) δ 11.76 (s, 1H), 7.45 – 7.27 (m, 5H), 7.17 – 7.09 (m, 1H), 6.96 (d, *J* = 7.5 Hz, 1H), 6.88 (d, *J* = 8.1 Hz, 1H), 6.74 (t, *J* = 7.4 Hz, 1H), 4.42 (s, 1H), 3.77 (dt, *J* = 10.6, 7.0 Hz, 4H), 2.71 – 2.37 (m, 4H).

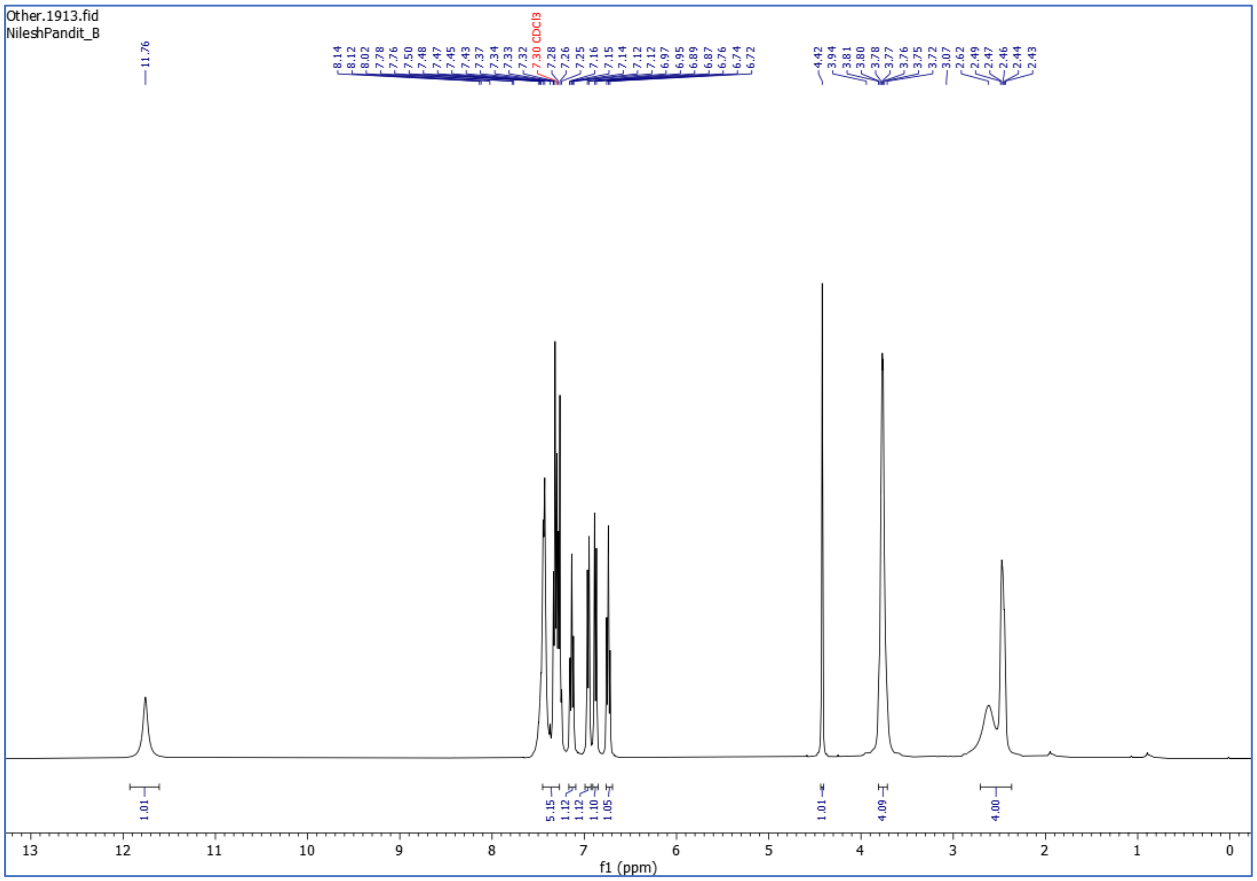

Fig. 18 ^{1}H NMR spectrum of 2-(morpholino(phenyl)methyl)phenol

^{13}C NMR

^{13}C NMR (101 MHz, $CDCl_3$) δ 156.05, 139.24, 129.41, 128.95, 128.71, 128.52, 128.14, 124.77, 119.63, 117.04, 76.83, 66.90, 52.23.

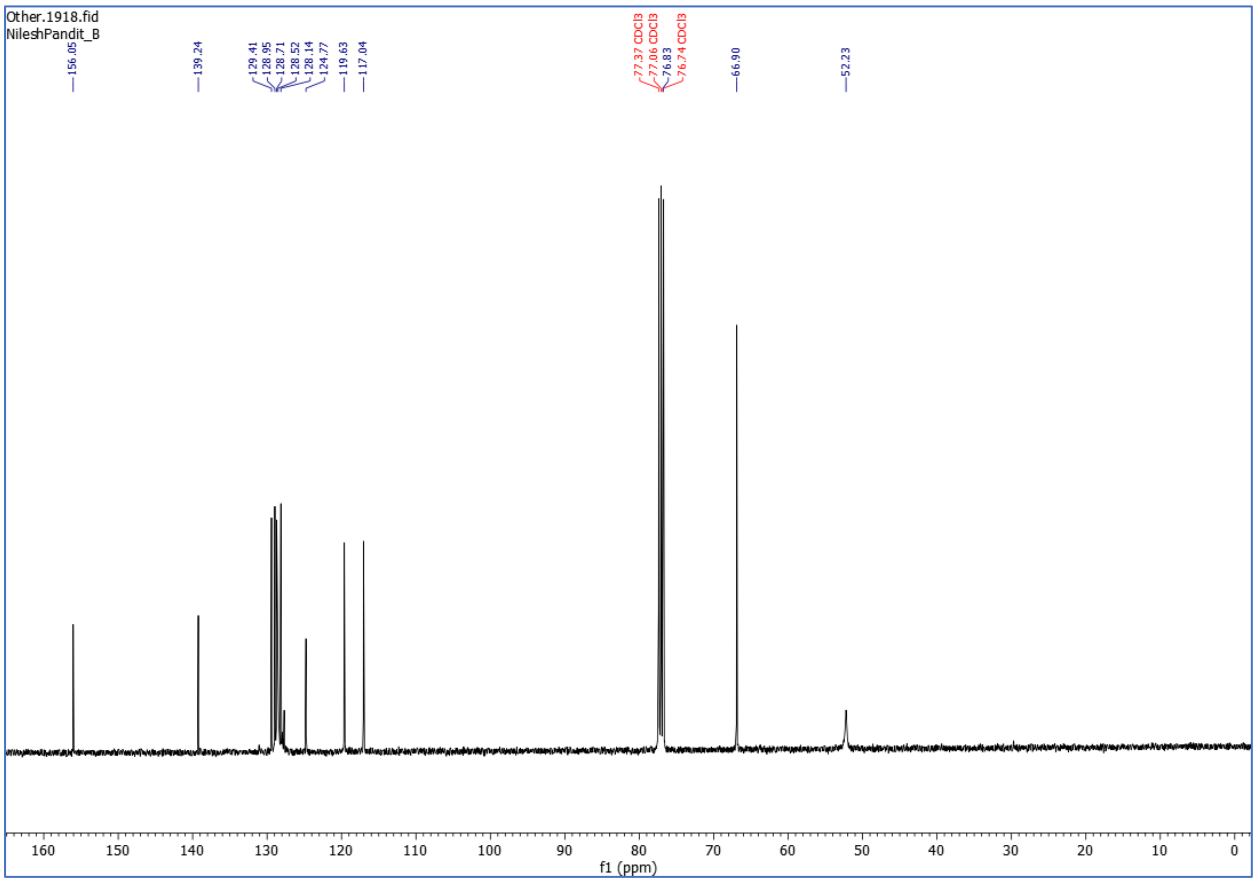

Fig. 19 ^{13}C NMR spectrum of 2-(morpholino(phenyl)methyl)phenol

References:

(1) Kekessie, I.; Wegner, K.; Martinez, I.; Kopach, M. E.; White, T. D.; Tom, J. K.; Kenworthy, M. N.; Gallou, F.; Lopez, J.; Koenig, S. G.; Payne, P. R.; Eissler, S.; Arumugam, B.; Li, C.; Mukherjee, S.; Isidro-Llobet, A.; Ludemann-Hombourger, O.; Richardson, P.; Kittelmann, J.; Sejer Pedersen, D.; Van Den Bos, L. J. Process Mass Intensity (PMI): A Holistic Analysis of Current Peptide Manufacturing Processes Informs Sustainability in Peptide Synthesis. *J. Org. Chem.* **2024**, *89* (7), 4261–4282. https://doi.org/10.1021/acs.joc.3c01494.

(2) Gómez-Biagi, R. F.; Dicks, A. P. Assessing Process Mass Intensity and Waste via an *Aza* - Baylis–Hillman Reaction. *J. Chem. Educ.* **2015**, *92* (11), 1938–1942. https://doi.org/10.1021/acs.jchemed.5b00249.